Edge detection and gravity sources depth estimation of southwestern Sirt Basin Libya, from gravity anomaly data

Hisham Nouri Elosta.

Geophysics Department - Faculty of Science – University of Tripoli

hi.elosta@uot.edu.ly

Omar Emhemed Omar Omran.

Higher Institute of Science and Technology - Kikla

Omaromar19755@gmail.com

Prof. Bashir M.Youshah

University of Tripoli - Faculty of Science

bashir.1962.bb@gmail.com

ABSTRACT

Understanding the subsurface geologic structure of a region often require indirect geophysical approaches; this study delineates the edges and estimates the depths of gravity source bodies to achieve this for the study area. The gravity data was provided by the Libyan Petroleum Institute. Low-pass filters were used to separate the residual and regional components of gravity dataset, while the horizontal gradient magnitude (HGM), tilt derivative ratio (TDR), and the analytic signal ration(AS) methods were applied to delineate and estimate the depth of gravity source bodies. The study area is located in the Southwestern part of Sirt Basin, Libya. Spectral (matched filtering) analysis of the Bouguer gravity anomaly reveals to equivalent layers with some additional noise, corresponding to shallow and deep density contrasts with mean depths of 2.5km and 8.5km respectively.by applying the horizontal gradient magnitude and tilt derivative methods to the Bouguer anomaly map, distinct geologic trend faults were identified along the NE-SE, N-S, and NW-SE directions, with the NW-SE trend corresponding to the Gattar Ridge structure. Additionally, analytic signal depth estimates (0.4-5km; mean 2.7km) closely match the matched filter depth of 2.5km, reinforcing the result. The combined appraisal of source edge locations and gravity source depth estimates offers useful information on underlying basement configuration, which is highly essential for exploration targets that are mostly obscured.

الملخص .

غالباً ما يتطلب فهم البنية الجيولوجية تحت السطحية لمنطقة ما استخدام أساليب جيوفيزيائية غير مباشرة؛ و تهدف هذه الدراسة إلى تحديد حدود الاجسام المولدة للشذوذ الجاذبية و تقدير أعماقها لتحقق ذلك في منطقة الدراسة. تم توفير بيانات الجاذبية من قبل معهد النفط الليبي. استخدمت المرشحات ذات التمرير المنخفض لفصل المكونين الإقليمي و المتبقي من بيانات الجاذبية، في حين تم تطبيق طرق حجم التدرج الافقي، و نسبة المشتقة المائلة، و نسبة الإشارة التحليل لتحديد حدود الاجسام المولدة للجاذبية و تقدير أعماقها. تقع منطقة الدراسة في الجزء الجنوبي الغربي من حوض سرت، ليبيا. أظهر التحليل الطيفي لشذوذ بوجير الجاذبي و جود طبقتين مكافئتين مع بعض الضوضاء الإضافية، تقابلان تباينات كثافة ضحلة و عميقة بمتوسط عمق 2.5كم . 8.5كم علي التوالي. و بتطبيق طريقتي حجم التدرج الافقي و المشتقة المائلة على خريطة شذوذ بوجير، تم تحديد اتجاهات جيولوجية مميزة للصدوع بامتداد شمال شرق-جنوب شرق، و شمال- جنوب، و شمال غرب- جنوب شرق، حيت يتوافق الاتجاه الأخير مع تركيب قتاره ريدج. كما أظهرت تقديرات العمق المستخلصة من الإشارة التحليلية (بمدى 0.4-5كم و متوسط 2.7كم) توافقاً وثيقاً مع عمق 2.5كم الناتج عن المرشح المتطابق، مما يعزز صحة هذه النتيجة.

يوفر التقييم المشترك لموقع حدود المصادر و تقديرات أعماق مصادر الجاذبية معلومات مفيدة حول تكوين القاعدة الصخرية الأساسية، و هو أمر بالغ الأهمية لأهداف الاستكشاف التي تكون في معظمها غير مكشوفة.

Received: 25-01-2026 - Accepted: 15-02-2026 - Published: 02-03-2026

Keywords Sirt Basin, Match filtering, Horizontal gradient magnitude, Tilt derivative, Analytic signal .

الكلمات المفتاحية : حوض سرت , الترشيح المطابق , مقدار التدرج الافقي , مشتقة الميل والاشارات التحليلية .

1- Introduction

Subsurface geological investigation have extensively relied on the application of gravity data. Various techniques based on the frequency analysis of the gravity field have been established to define parameters such as the location of boundaries and the depths of the density contrasts that cause anomalies in the gravity field (Salem et al., 2008). The horizontal gradient magnitude is one such method used for locating contacts and faults from gravity anomaly data (Cordell et al.,1985; Phillips, 2000). Additional methods for delineating source edges and estimating source depths including the analytic signal (Nabighian, 1972; Roest et al., 1992) and tilt derivative (Miller et al., 1994; Verduzco et al., 2004). By analyzing variations in rock density through gravity data, derivative methods enable indirect subsurface imaging and facilitate the delineation of buried tectonic structures essential to hydrocarbon exploration. Consequently, these methods are consistently applied to interpret gravity anomaly data to obtain the information needed for hydrocarbon exploration (Muzaffer et al., 2013).

This study focuses on the southwestern region of the Sirt Basin which is a significant geological feature characterized by its rift basin architecture, formed on a foundation of Pan-African to Paleozoic basement rocks. This basin has complex tectonic and sedimentary structures. The basin's tectonic evolution was characterized by multiple rift episodes, primarily during the Mesozoic and Cenozoic, resulting in substantial subsidence and deposition of thick sedimentary sequences (Abdunaser & McCaffrer, 2014). As interest in more robust subsurface imaging and structural interpretation methods.

The study utilizes gravity anomaly data obtained from Libyan Petroleum Institute to identify subsurface geological structures of potential significance for future exploration. We used derivative-based and matched filtering methods to estimate source depths and delineate edges of the gravity source contrast. The study area (Fig. 1) is geographically situated between latitude 27° 30' to 28° 30' N and longitude 17° 30' to 18° 20' E covering an area of approximately 9000km^2. The resulting depth to the basement map, that is the depth to the density contrast interface representing the basement beneath the study area, provides a guide for suture exploration projects.

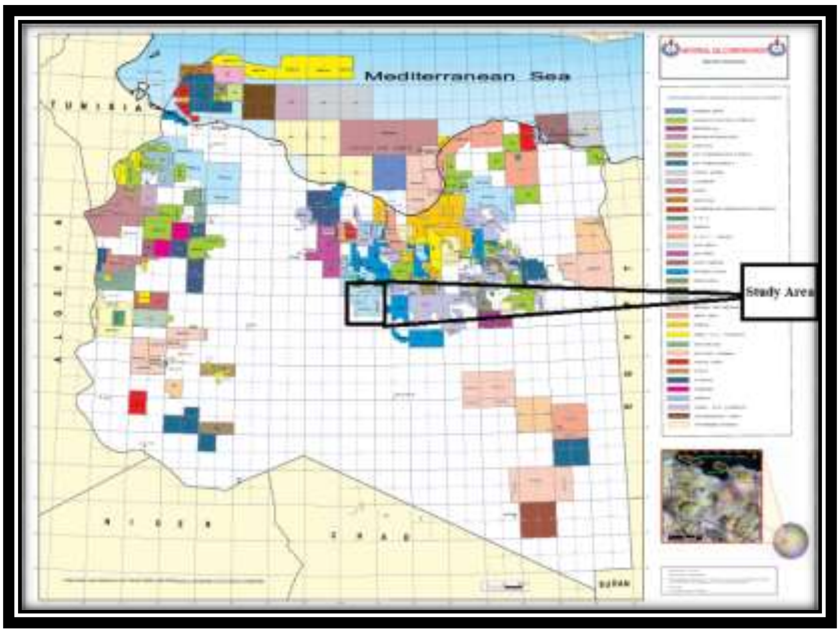

Fig. 1: Location map of the study area

2- Geological setting

The Sirt Basin in Libya is a significant geological feature characterized by its rift basin architecture, formed on a foundation of Pan-African to Paleozoic basement rocks. This basin is complex tectonic and sedimentary structures (Fig. 2).

2.1 Geological Structure and Tectonics

- The Sirt Basin exhibits a northwest-southeast trending structure influenced by tectonic movements that have shaped its rift architecture (Abdunaser & McCaffrer, 2014).
- The Sirt Basin has undergone multiple tectonic phases from the Late Jurassic to the present, characterized by periods of rifting and subsidence. These phases are crucial for understanding the basin's evolution and are consistent with tectonic activities in other African basins (Abadi et al., 2008).
- The basin's development is influenced by its orientation and underlying basement structure, which control the rifting and reactivation processes. This structural complex is reflected in the gravity data, which helps in delineating the basin's tectonic features (Abadi et al., 2008).
- The Sirt Arch was created during the Hercynian Orogeny from inversion of the Kalansgiyu Tough and early Paleozoic tectonic structure. Rifting in the Sirt Basin likely began in Triassic with varying opinions on its continuation and timing of tectonic events.
- The Sirt Basin underwent an anticlockwise rotation of axis through time from NE-SW Early Cretaceous through N-S Upper Cretaceous to NW-SE Paleocene and Eocene (Saleem 2015).

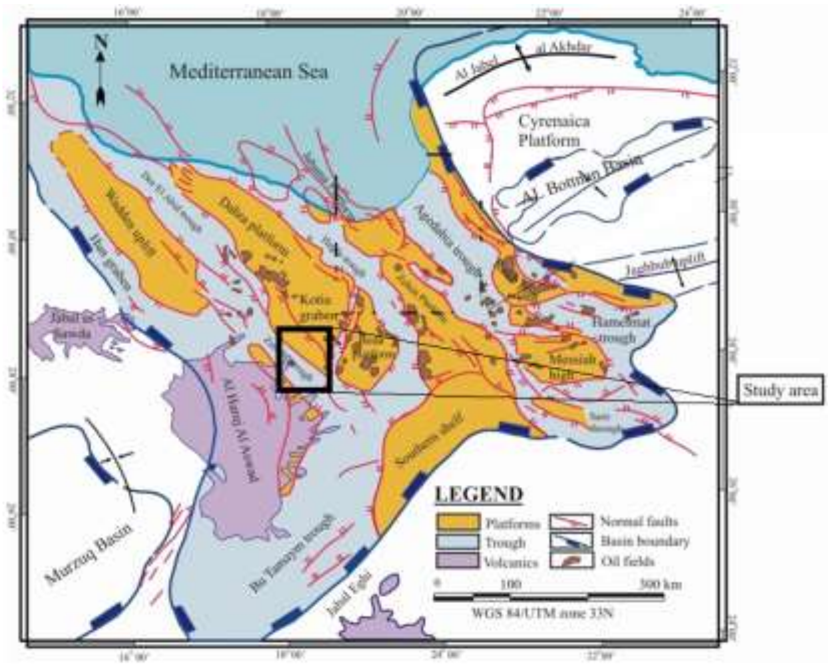

Fig. 2 Major structure elements of Sirt Basin Libya showing the study area (modified after, Roohi. M., 1996)

2.2 The Main Tectonic Phases in Sirt Basin

- Post-Pan African orogeny and Paleozoic sedimentation: Initial basin Involved sediments deposited after the Pan-African orogeny, followed by uplift, faulting, and erosion during the Hercynian Orogeny, which inverted earlier structures to form the Sirt Arch (Saleem 2015).
- Triassic to Early Cretaceous rifting: Incipient rifting began in the Triassic, with limited extension that continued into the Early Cretaceous, leading to the formation of troughs, platforms, and the collapse of the Tibisti-Sirt Arch (Saleem 2015).
- Cretaceous extension and marine transgression: From the Aptian through the Cenomanian, continued extension, block faulting, and marine transgressions led to the development of sediments like the Sirt Shale and the formation of pull-apart grabens controlled by NW-SE fracture zones (Saleem 2015).
- Rift-infill and post-rift subsidence: During the Maastrichtian, rift infill persisted until the basin experienced significant sag subsidence, with ongoing tectonic activity leading into the final stages of the Cenozoic.
- Cenozoic tilting and basin rotation: In the late Cretaceous to Cenozoic, the Sirt Basin axis rotated anticlockwise, and the basin experienced northeast tilting, subsidence, and basin inversion influenced by the relative motion of Africa with respect to Eurasia (Saleem 2015).

3- Methods

This investigation utilized a high resolution gravity anomaly map, made available by the Libyan Petroleum Institute (LPI) and acquired in 2024 by the Geophysics Department, Faculty of Science, University of Tripoli. The gravity data cover a part of the southwestern Sirt Basin (Fig. 3). The Bouguer gravity anomaly was enhanced to image subsurface geologic structures of the study area by applying several standard derivative and matched filtering techniques. All processing was performed using the software packages Oasis Montaj (Geosoft, 2015) and ArcGIS (Esir, 2019) to produce the Bouguer, Regional and Residual maps. Several filtering techniques were applied, including Matched Filtering, Upward Continuation, Horizontal Gradient Magnitude (HGM), Tilt Derivative Ration (TDR), and Analytic Signal (AS).

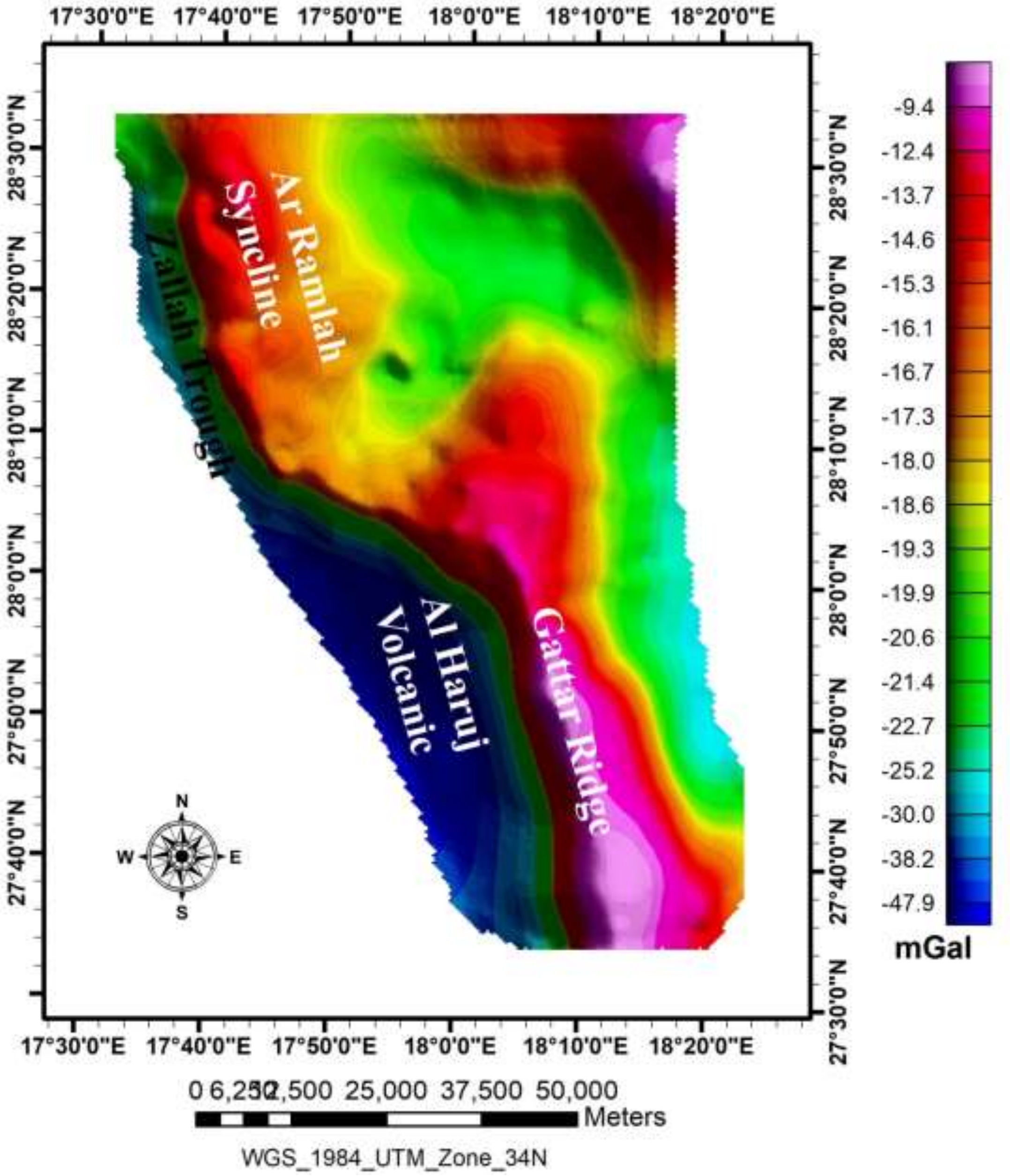

Fig. 3 Bouguer gravity map of the study area

3.1 Regional residual separation using matched filtering

Matched filtering is a useful technique for separating gravity anomalies originating from sources at different depths. The method is based on the interpretation of the radially averaged power spectrum of the Bouguer gravity map, in which straight-line segments are fitted to the spectral curve. Each linear segment is assumed to represent an equivalent layer of subsurface sources at a specific depth within the study area (Sheriff, 2010).

For the study area, the radially averaged power spectrum (Fig 4a) can be subdivided into three linear segments, each corresponding to a distinct subsurface gravity source layer.

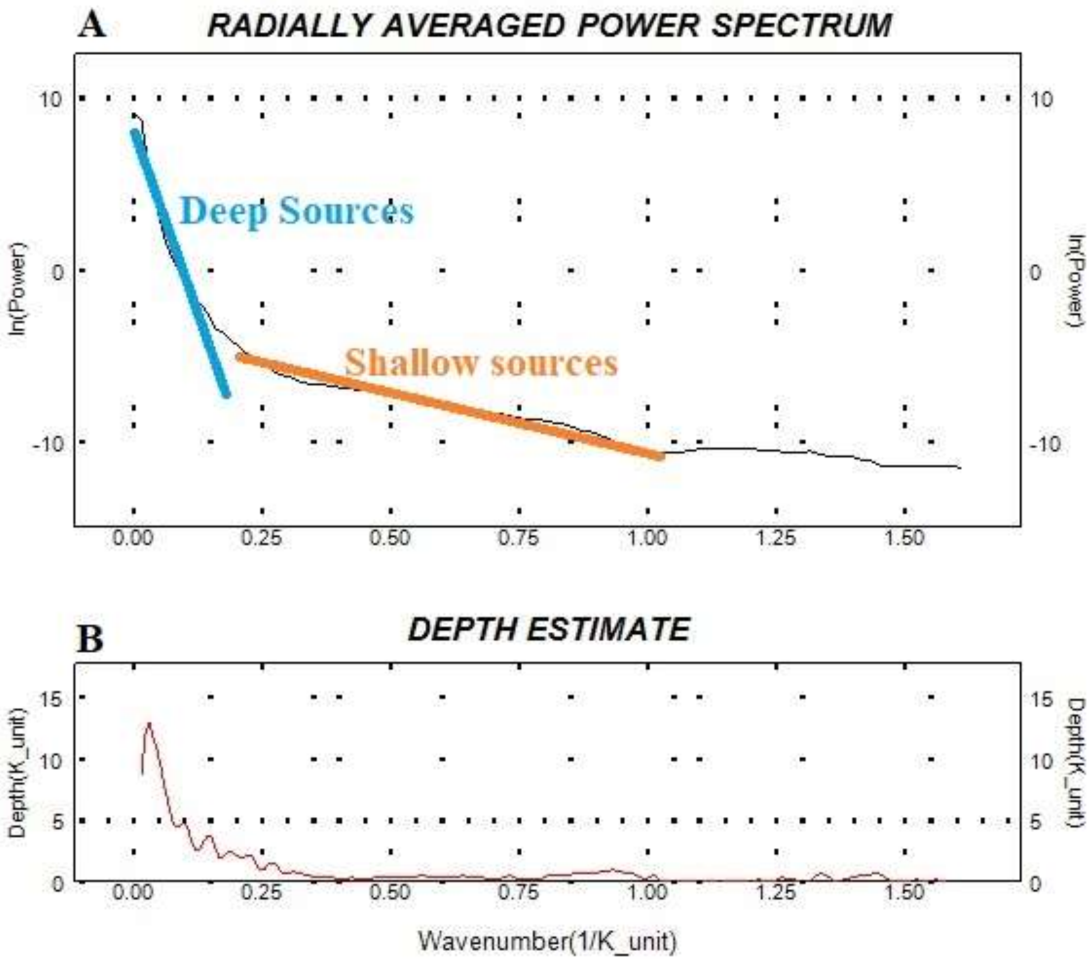

Fig. 4 A. Average power spectrum plot of the Bouguer gravity map of study area, B. depth estimates for gravity sources based on linear segments of the power spectrum curve.

After the depth levels have been identified, the individual anomaly components may be separated from the Bouguer gravity map using band-pass filtering, such as a Butterworth filter. Butterworth filters are particularly useful because they permit convenient control of the low-pass and high-pass responses while maintaining a fixed central wavenumber. When ringing artifacts are observed, the filter order is commonly reduced to improve the quality of the result. The depth to the top of each subsurface layer fig 4b is then estimated from the slope of the corresponding linear segment of the power spectrum using the appropriate relationship between slope and depth.

$$Z(depth) = \frac{-slope}{4\pi} \ldots \ldots \ldots \ldots .(1)$$

The low-pass filter was applied to the Bouguer gravity data to allow short wavenumbers (low frequencies) to pass to the output channel. Features in the data that are shorter than the short wavelength cutoff will removed. This processing employed to separate gravity field data into regional and residual anomalies. The regional anomaly corresponds to deep, long-wavelength features usually associated with large scale geological structures, while the residual anomaly reveals shallower, smaller scale anomalies from localized sources. By subtracting the regional anomalies figure 5A from the Bouguer map to get the residual anomalies figure 5 **B.**

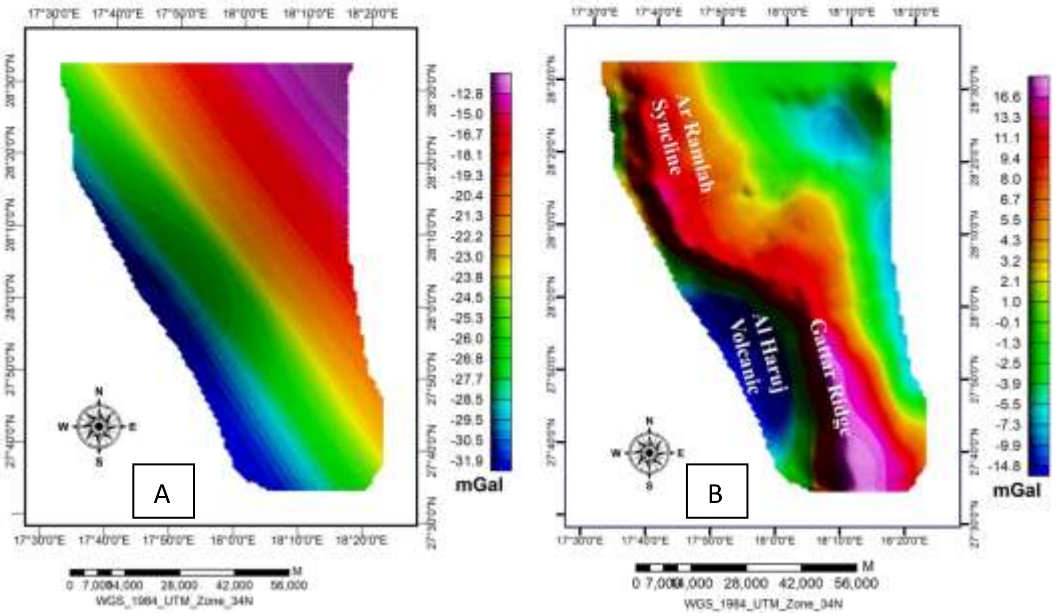

Fig.5 A Regional gravity anomaly map, B Residual gravity anomaly map of study area

3.2 Edge detection methods

Edge detection methods are essential tools for delineating the edges of boundaries and consequently, the horizontal extent of subsurface gravity sources bodies. These boundaries may represent fault offsets, lithological contacts, or other abrupt change in rock density.

3.2.1 Horizontal gradient magnitude (HGM)

The horizontal gradient magnitude (HGM) is used to identify the edges of gravity sources. It is defined as the vector magnitude of the first-order horizontal derivatives of the gravity field in the x and y directions. It enhances short-wavelength lateral variations associated with density contrasts while reducing its regional trend along that direction. In general,

The HGM commonly attains local maxima over or near the edges of geological bodies where the lateral density contrast is greatest. The maximum value of horizontal gradient can be a straightforward technique highlighting potential edges of subsurface gravity source bodies, lithological contacts, and faults (Cordell L, 1985; Roest, 1993). When horizontal gradient maxima are aligned linearly, it can be interpreted as a linear contrast in gravity properties, the edges of a gravity sources body. This technique therefore involves identifying locations where the local maxima in the HGM are aligned, and gravity sources body edges may be interpreted at these locations. Note that the maxima of horizontal gradient are strongest when the edges are oriented vertically, edges that deviate too far from vertical do not result local gradient maxima. Due to the necessity of computing the two first order horizontal derivatives of gravity field for the HGM method, the technique is immune to gravity data noise (Phillips JD 2000). If g(x,y) represents the gravity at the location (x,y) the HGM is provided as:

$$HGM(x,y) = \sqrt{\left(\frac{\partial g}{\partial x}\right)^2 + \left(\frac{\partial g}{\partial y}\right)^2} \text{.........(2)}$$

Where the horizontal derivative are $\partial g/\partial x$ and $\partial g/\partial y$ of the gravity data. The HGM was calculated for the Bouguer gravity map of the study area. Peaks of the HGM were extracted by moving a 3x3 window across the grid and identifying local maxima, following the edge- detection procedure (Blakely & Simpson, 1986).

3.2.2 Tilt derivative (TDR) method

The Tilt Derivative Ratio (TDR) is an advanced edge detection technique that combine the tilt angle with vertical and horizontal derivative of the gravity field. This technique is applied to map shallow geological structures because it is particularly effective at identifying the edges of gravity source bodies. The technique was first presented by Miller and Singh (Miller & Singh,1994), then it was subsequently advanced by Verduzco et al (Verduzco et al, 2004), who provided it as:

$$TDR = \tan^{-1}\left(\frac{VDR}{HGM}\right) \text{.........(3)}$$

Where the vertical derivative is denoted by VDR, and the total horizontal derivatives are denoted by HGM.

The tilt angle derivative amplitudes lie in the interval from -90º to +90º [-π/2 and +π/2], regardless of the amplitude of VDR or the absolute value of HGM (Verduzco et al., 2004; Salem et al.,2007). Not that, TDR amplitudes are positive over gravity source bodies and negative outside them, with the zero contour indicating the sources' edges (Miller & Singh, 1994;Verduzco et al., 2004; Cooper, 2009) this sign convention follows from that the first vertical derivative of a gravity anomaly is positive above a density contrast (source) and negative outside it, whereas the horizontal gradient reaches its maximum near the edges, consequently, the arctangent ratio produces positive angles over the source, crosses zero at the edges, and turns negative beyond them (Askari et al.,2021)

3.3 Depth to basement estimation

3.3.1 Analytic signal (AS) method

The analytic signal (AS) method enhances gravity data interpretation by detecting edges and estimating source locations of subsurface density anomalies. It processes Bouguer gravity anomalies to compute horizontal and vertical gradients, forming a complex valued signal whose amplitude maxima pinpoint anomaly sources. The magnitude of the analytic signal AS is described by (MacLeod, 1993) in Eq. (4)

$$AS = \sqrt{\left(\frac{\partial g}{\partial x}\right)^2 + \left(\frac{\partial g}{\partial y}\right)^2 + \left(\frac{\partial g}{\partial z}\right)^2} \text{......... (4)}$$

Where g is the gravity field and derivatives are obtained via finite differences. Maxima in AS amplitude indicate source edge independent of magnetization direction(unlike magnetic data), making it suitable for noisy gravity datasets.

One of advantage of the analytical signal method is useful in gravity interpretation because it helps locate density contrasts and subsurface structures without requiring many assumptions about the source. It is especially helpful for identifying the edges and positions of bodies such as faults, contacts, steps, cylinders, sills, and compact masses. In these cases, the analytical signal produces a symmetric peak directly above the source, making it useful for mapping gravity anomalies and structural boundaries (Nabighian, 1972 and Roest,1992).

The depth to the gravity source is determined by the ratio of the analytic signal of the residual gravity data (AS) to the first vertical derivative of analytic signal of the residual gravity data (AS1) as presented in Eg. 5

$$AS1 = \sqrt{\left(\frac{\partial FVD}{\partial x}\right)^2 + \left(\frac{\partial FVD}{\partial y}\right)^2 + \left(\frac{\partial FVD}{\partial z}\right)^2} \quad \text{......... (5)}$$

Where:

FVD represents the first vertical derivative of the residual gravity data.

The depth to the gravity sources are estimated using the following relation

$$D = \frac{AS}{AS1} * N \text{........(6)}$$

Where:

D is the depth to the gravity sources, N is the sturcural Index which depends to the geometery of the gravity sources. For example, N= 2 for a spheare, N= 1 for horizontal cylinder, and N= 0 for fault or thin sheet (Reid el al., 1990)

4- Result and discussion

The Bouguer gravity map of the study area (fig. 3) depicts gravity anomaly values between -47.9 to -8 mGal. the Bouguer gravity map shows prominent low density (negative) values distributed at the northeastern and southwestern parts of the map with NW-SE and N-S trends which indicate lower density beneath the measurement point. The NW-SE trend is the most prominent and is associated with major fault zone, grabens, and shear zones that reflect extensional tectonic related to rifting phases in the Sirt Basin's history. These faults strongly influence sediment thickness distribution and structural segmentation of the basin. The Bouguer gravity map indicate the Zallah Trough as a deep fault bounded depression with prominent N-S trending. Furthermore, the southern part of Zallah Trough, which is close to Al Haruj Volcano, chractrized by gravity low that varies between -28 and -19 mGal. This anomaly is probably due to both intrusive and extrusive of the Al Haruj volcanic activities. In addition the Bouguer gravity map highlights high –amplitude anomalies, particularly the structural characteristics of the Gattar Ridge's and the Ar Ramlah Syncline, mainly by illustrating alterations in gravity associated with faults that trend NW- SE direction .

In order to investigate the subsurface geological structures, we applied the matched filtering technique to the Bouguer gravity map to determine the depths of the main source bodies in the study area. The average power spectrum curve for the Bouguer gravity map of the study area shown in Fg. 4, which used to separate the regional and residual sources and also to define the noise. The depth estimate map that resulted was used to determine the average depths to the tops of the deep and shallow anomalies. While the shallow sources are about 0.5 to 4km, and the depth to the top of deep sources is about 5 to 12km (fig. 4). The linear sections (blue and red) in fig 4a are used to define the cut off wavelength that separates the shallow and regional anomaly sources, which correspond to depths of about 500m and 5000m from the top of the shallow and regional sources, respectively.

The regional gravity map (fig. 5A), low-pass filtered at 50km cutoff wavelength, reveals long wavelength subsurface density variation across study area. Gravity values range from highs near -11 mGal in the north to lows of -32 mGal South, indicating thick low density sedimentary basins overlying denser basement.

The residual gravity map (fig. 5B) corresponds to short wavelengths fields of shallow bodies, which was the result of simple subtracting of the low pass anomaly map, which is the regional anomaly map from the Bouguer anomaly map. The residual gravity map shows positive and negative gravity sources of various wavelengths and amplitudes with values, which range from -17.2 to 18.3 mGal. The distribution of anomalies is similar to the Bouguer anomaly map Visual analysis of the residual gravity map indicates that the map was characterized by negative anomaly in the northern part dominant N trend which reveals anomalies over Zallah Trough, and positive anomaly in the southern part dominated NW-SE trending which reveals the Ar Ramlah Syncline and the Gattar Ridge's structural.

Tilt derivative (TDR) filtering is widely used for identifiting and delineating geological structures, especially those linked to shallow basement strructural features or mineral exploration targets. The TDR filter was applied to the Bougure anomaly data, to provide greater resolution of structural features. The TDR map (fig. 6) demarcates possible edges of geologic source bodies. The TDR tethnique facilitates the horizontal location with the extent of edges of gravity source bodies within the study area. When utilizing the gravity anomaly data, the TDR is positive (orange and magnta colors) when is is over gravity sorces bodies and is negative (blue and gran colors) when it is outside the gravity sorves bodies. The zero contours on the TDR map mark the positions of sharp lateral changes in density contrast, i.e., the contact boundaries between adjecent positive and negitive gravity source bodies. As a result, the contact boundary or edges of gravity source bodies are represented by the zero contours on the TDR map and also, indicated by the transition from grean to yellow color. The gravity source bodies delimited on the TDR map exhibit the same overall pattern as Bouguer gravity map, which highlights the major fault systems on the study area; these source bodies are linear and trend NW-SE, representing internal deformation features associated with later tectonic adjestments.

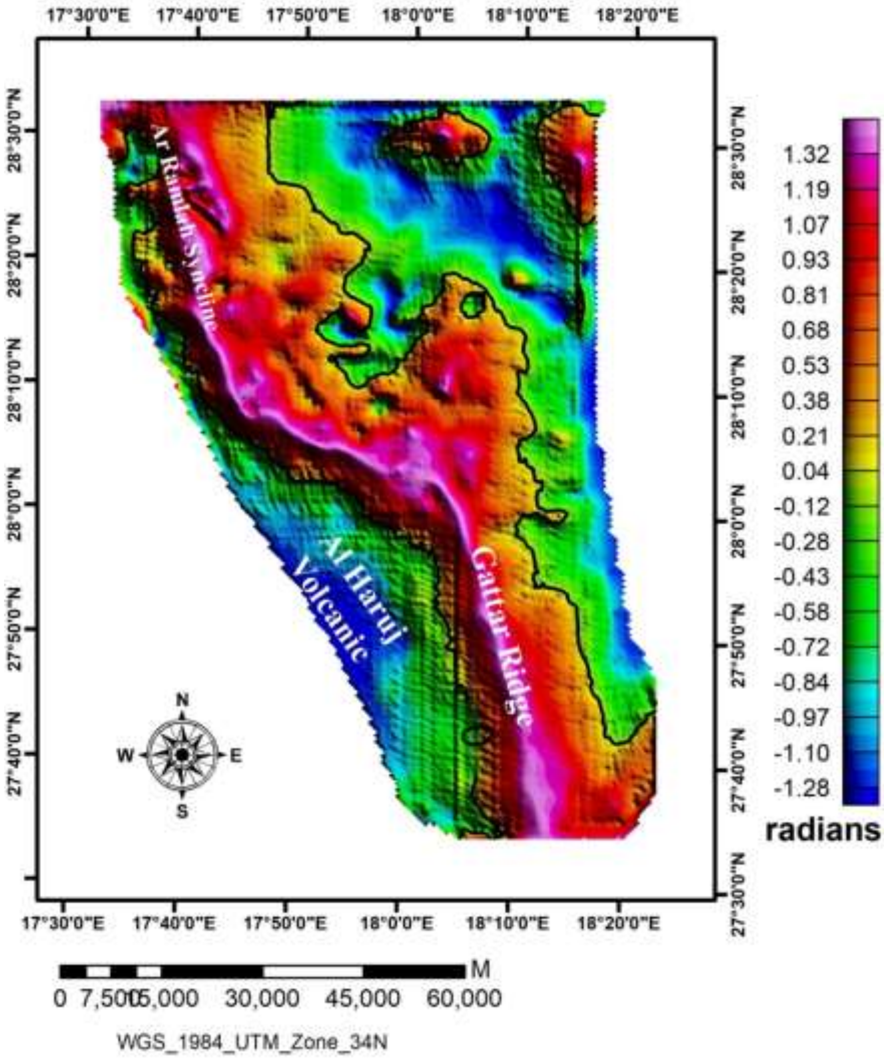

Fig.6 Color-shaded TDR map of Bouguer gravity anomaly data of study area

The horizontal gradient magnitude (HGM) was applied on the Bouguer gravity anomaly data of the study area, as an additional method to detect the edges of gravity sources, which is shown in fig. 7.Geologic fault trends striking NE-SW, N-S, and NW-SE where delineated, with the NW-SE trend associated with the Gattar Ridge structure. Long linear peak of the horizontal gradient magnitude of the Bouguer anomaly data delineate the edges of gravity sources. This peak is sketched quantitatively using the procedure described in the methods section. There is a very good correlation that can be seen between the peak of HGM and the zero contour lines of the TDR for the main features of the anomaly map. This correlation indicates that both methods define the same primary structural boundaries within the study area. HGM peaks are donated as red lineaments, and TDR zero contours are donated as black lineaments, as seen in fig. 8

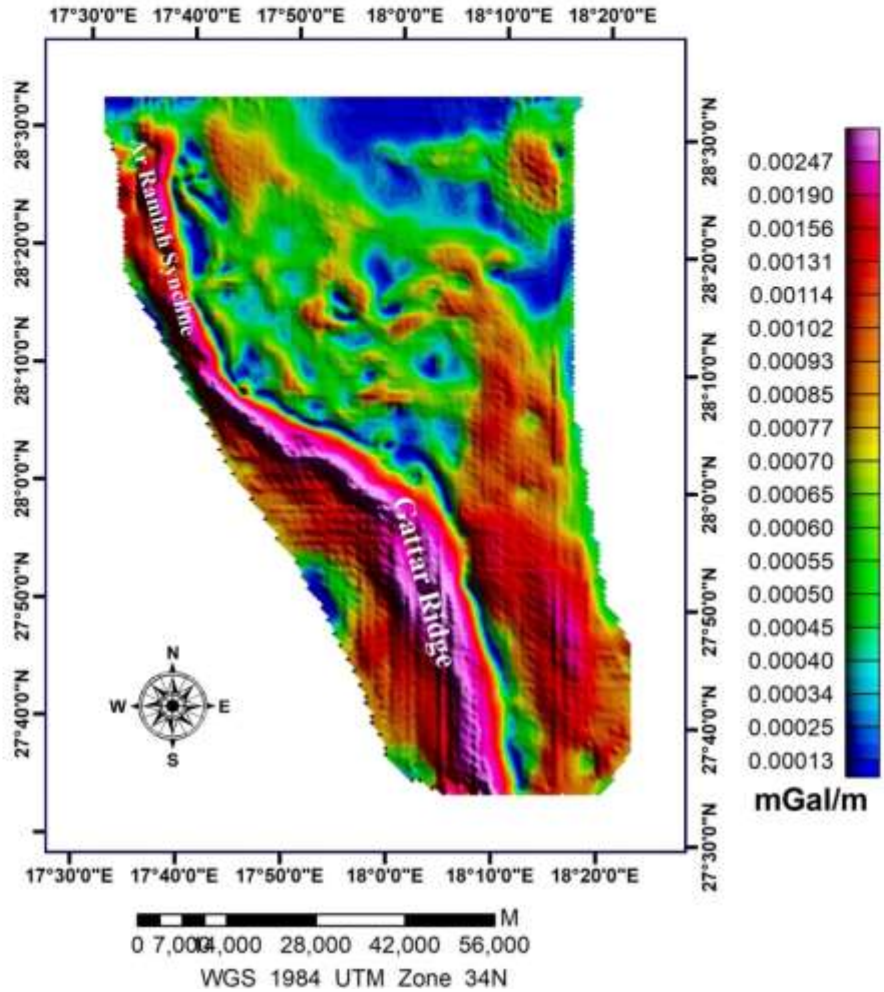

Fig. 7 Color-shaded Horizontal gradient magnitude map of Bouguer gravity anomaly data of study area.

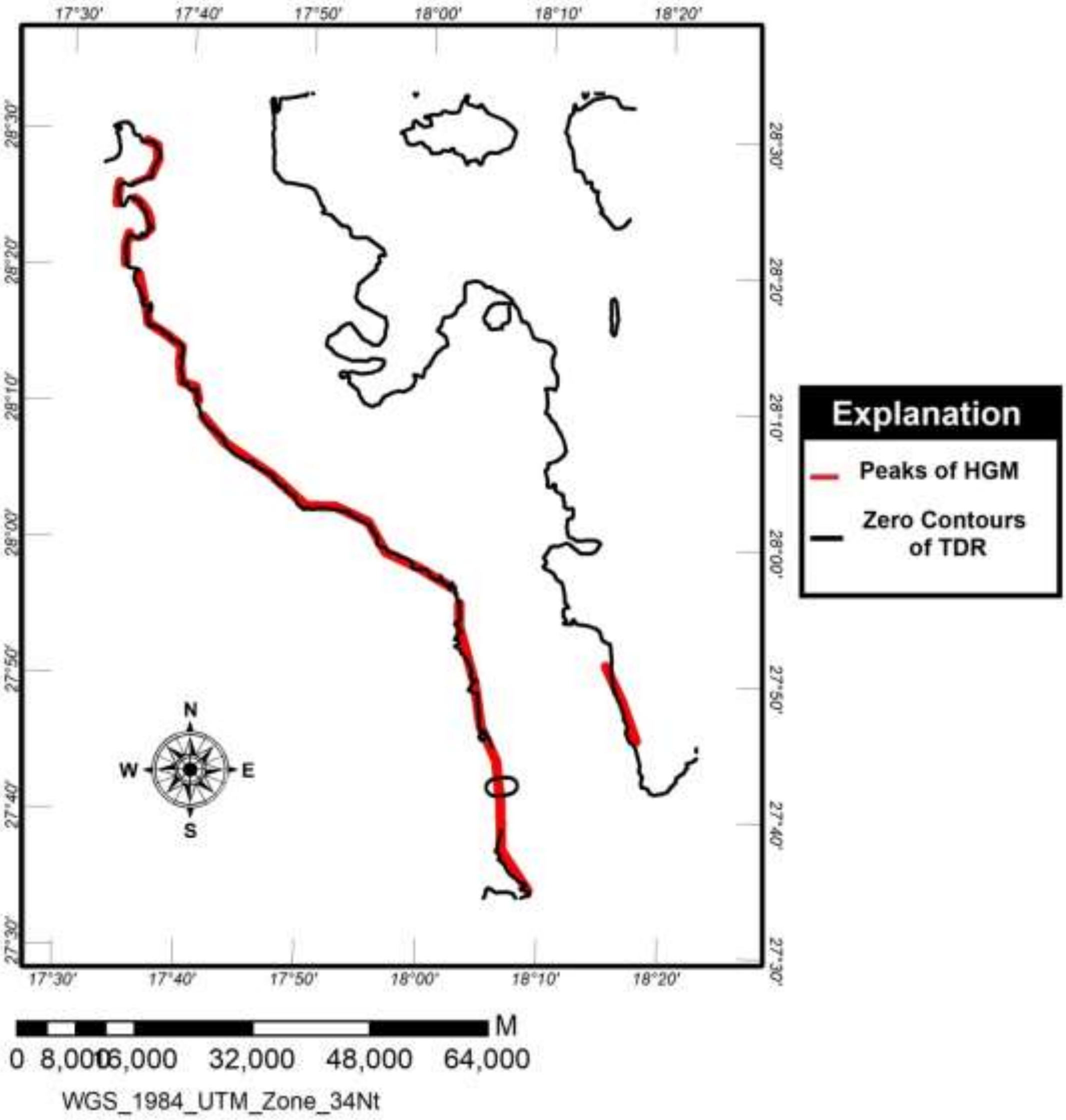

Fig.8 Peaks of HGM plotted on TDR map of the study are, the HGM peaks are located on Zero contour lines of TDR map.

The analytic signal (AS) technique was applied to infer the configuration of the gravity basement beneath the study are. Thus technique enhances the detection of subsurface density variations. From Eq. 6, the analytic signal of the Bouguer gravity map (AS) was divided by the analytic signal of the first vertical derivative of Bouguer gravity map (AS1) to properly produce the gravity basement depth map of the study are (Fig.9). the resulting depth map reveals the spatial distribution of gravity source bodies at different depths, offering greater detail than the matched filter results. Overall, the estimated depths range from 450 m to 5000 m. depth variations are shown using a color gradient. Blue and green indicate shallow sources at depths less than 2000m which is in reasonable agreement with the radially average power spectrum estimate (Fig. 4). In contrast, red and magenta indicate deeper sources, with depths up to approximately 5000m.

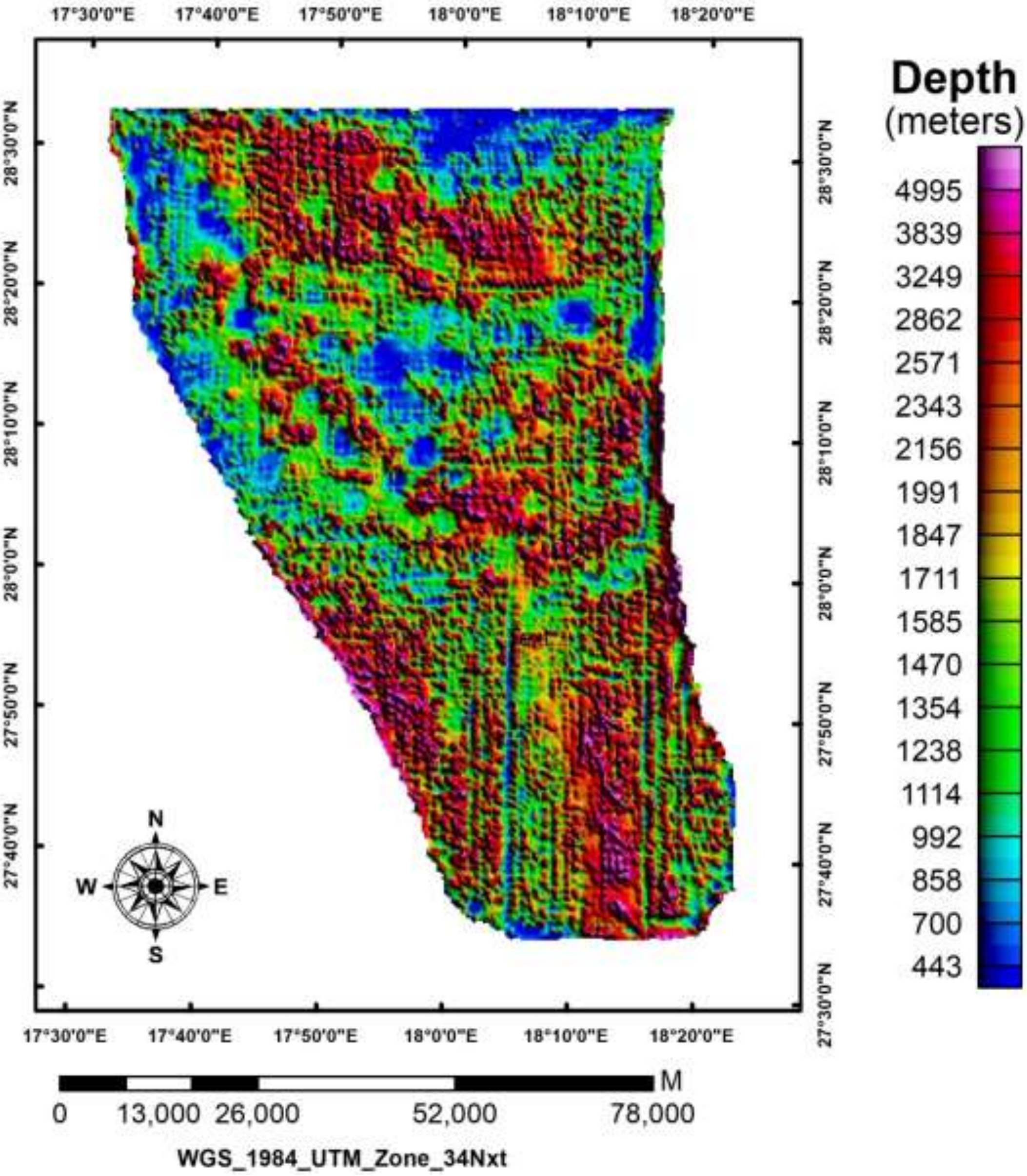

Fig. 9 Depth to the gravity sources map deduced using the analytic signal method

5- Conclusion

In this study, gravity data were used to investigate the subsurface geology of the area, with the aim of delineating the edges and estimating the depths of the gravity sources responsible for the geologic structure.

By applying standard interpretation techniques to the Bouguer anomaly map, several key subsurface features were identified, including the edges of gravity source bodies and the depths of shallow and deep gravity sources were estimated. The Bouguer gravity map reveals a subsurface structure dominated by NW-SE and N-S trending low density zones, with the NW-SE trend reflecting major faults, graben, and shear zones associated with extensional rifting history of the Sirt Basin. High-amplitude anomalies along the Gattar Ridge and Al Ramlah Syncline, both linked to NW-SE trending faults, further underscore the strong structural and tectonic control exerted on the region's gravity signature. The horizontal gradient magnitude (HGM) and tilt derivative ratio (TDR) technique were applied to the Bouguer anomaly map, and the strong correlation between the two methods provided robust delineation of the edges of gravity sources. Both methods consistently identified the same primary structural boundaries, thereby confirming a dominant NW-SE trend across the study area. The depth estimation methods employed differ in their approach to characterizing subsurface structures: radial power spectrum analysis estimates the average depths of gravity source ensembles from spectral slopes, whereas the analytic signal method provides higher resolution information on local source boundaries and depth variation. The depths obtained through these methods range from 400 to 5000 m, with an average depth of approximately 2400 m. Collectively, these findings provide valuable insights into the structural framework of the study area establish a foundation to future exploration research in the area.

References

Abadi, A.M., Van Wees, J.D., Van Dijk, P.M., and Cloetingh, S.A.P.L. (2008) Tectonics and subsidence evolution of the Sirt basin, Libya. AAPG Bull., vol. 92 (8): p. 993–1027.

Abdunaser, K.M, McCaffrey, K.J.W. (2014) Rift architecture and evolution: The Sirt Basin, Libya: The influence of basement fabrics and oblique tectonics. Elsevier, Journal of African Earth Sciences 100, p 203–226.

Askari, M. et al. (2021) Edge detection of gravity anomaly sources via the tilt angle, total horizontal derivative, total horizontal derivative of the tilt angle and new normalized total horizontal derivative. Applied Geophysics, 194, 104-459

Blakely RJ, Simpson RW (1986) Approximating edges of source bodies from magnetic or gravity anomalies. Geophysics 51(7):1494–1498

Cooper, G. R. J. (2009). The use of tilt angle in gravity and magnetic methods. New Surface 2009 – 15th European Meeting of Environmental and Engineering Geophysics

Cordell L, Grauch VJS (1985) Mapping basement magnetization zones from aeromagnetic data in the San Juan basin, New Mexico. In: Hinze WJ (ed) The utility of regional gravity and magnetic anomaly maps. Society of Exploration Geophysicists, pp 181–197

MacLeod, I. N., Jones, K. & Dai, T. F. 3-D (1993) analytic signal in the interpretation of total magnetic field data at low magnetic latitudes. Explore. Geophysics. 24, 679–688.

Miller HG, Singh V (1994) Potential field tilt: a new concept for location of potential field sources. J Appl Geophys 32:213–217

Muzaffer ÖA, Ünal D (2013) Edge detection of magnetic sources using enhanced total horizontal derivative of the tilt angle. Yer bilimleri 34(1):73–82.

Nabighian MN (1972) The analytic signal of two-dimensional magnetic bodies with polygonal cross-section: its properties and use for automated anomaly interpretation. Geophysics 37:507–517. https ://doi.org/10.1190/1.14402 76.

Phillips JD (2000) Locating magnetic contacts: a comparison of the horizontal gradient, analytic signal, and local wavenumber methods. In: SEG technical program expanded abstracts 2000, pp 402–405

Reid A. B. Allsop J. M. Granser H. Millett A. J. Somerton I. W., (1990), Magnetic interpretation in three dimensions using Euler deconvolution: Geophysics , 55, 80–91.

Roest WR, Pilkington M (1993) Identifying Remanent magnetization effects in magnetic data. Geophysics 58:653–659.

Roest WR, Verhoef V, Pilkington M (1992) Magnetic interpretation using the 3-D analytic signal. Geophysics 57:116–125

Roohi. M, 1996. First symposium of the sedimentary Basins of Libya: Geology of Sirt Basin, vol.II, pp 323-336.

Salem A, Williams S, Fairhead J, Ravat D, Smith R (2007) Tilt depth method: a simple depth estimation method using first-order magnetic derivatives. Lead Edge 26:1502–1505

Salem A, Williams S, Fairhead D, Smith R, Ravat D (2008) Interpretation of magnetic data using tilt-angle derivatives. Geophysics 73:L1–L10

Saleem M.A.(2015) Tectonic Evolution and Structural Analysis of South Western Sirt Basin, Central Libya, School of Geography, Earth and Environmental Sciences. University of Birmingham, Thesis.

Sheriff SD (2010) Matched filter separation of magnetic anomalies caused by scattered surface debris at archaeological sites. Near Surf Geophysics 8:145–150

Verduzco B, Fairhead JD, Green CM, MacKenzie C (2004) New insights into magnetic derivatives for structural mapping. Lead Edge 23:116–119